Assessment of MPPT Techniques During the Faulty Conditions of PV System

Krishna Naick BHUKYA[1], Kalyan CHATTERJEE[1], Tarun Kumar CHATTERJEE[2]

[1]Department of Electrical Engineering, Indian Institute of Technology (Indian School of Mines),
Sardar Patel Nagar, Hirapur, Dhanbad, 826004 Jharkhand, India
[2]Department of Mining Machinery Engineering, Indian Institute of Technology (Indian School of Mines),
Sardar Patel Nagar, Hirapur, Dhanbad, 826004 Jharkhand, India

krishnalalitha.b@gmail.com, kalyanbit@yahoo.co.in, tkcism@yahoo.com

Abstract. *The contribution of Distributed Generation (DG) systems like wind energy systems and solar Photovoltaic (PV) systems on the generation of electricity has increased. Out of these DG systems, the PV systems have gained wide popularity, because of the availability of solar energy throughout the day. Depending on the size of PV installations, a large number of PV modules can be interconnected in the form of series and parallel connection. Since a large number of modules are interconnected, it is possible for the faults in a PV array to occur due to the failure of protection system, which can cause damage to the PV module and also the decrease in the output power. This paper presents the tracking of a maximum power point under the faulty conditions of 12×5 PV array. The fault conditions that have been considered in the PV array are open circuit fault, line to ground, line to line and failure of bypass diodes. Perturb and observe, incremental conductance and fuzzy logic controller are the maximum power point tracking techniques that have been implemented. For each of the fault conditions, the results have been presented in terms of the maximum power tracked, tracking time and tracking efficiency.*

Keywords

Fuzzy logic controller, maximum power point tracking, PV system faults, tracking efficiency.

1. Introduction

The extensive research work in the area of solar Photovoltaic (PV) cells has not only improved their efficiency but also reduced their cost. Irrespective of any geographic location, the availability of solar energy throughout the year, production of clean energy and reduction in manufacturing cost has led the policy makers to utilize solar PV systems on a large scale for the generation of electrical energy. And for the mass generation of electrical energy, a large number of PV modules is required, which are interconnected in the form of series and parallel connection. Due to the large size of PV installations, there are certain technical issues like faults that, if left unsolved, can cause a hindrance in the utilization of electrical energy from the operational point of view. Depending on the location of the fault, the fault analysis of PV system may be categorized into three types: PV array faults, failure of power conditioning units and the fault between the utility and PV array [1]. Failure of PV modules, line to ground and line to line faults are the faults in PV farm, which cause damage to the PV panels resulting in huge loss of energy [2].

The other common faults that lead to the failure of PV modules are open circuit fault, arc fault, formation of hot spot, mismatch of polarity, failure of bypass diode and the formation of dust/soil [3], etc. In addition to this, the power generated by the PV system also gets affected due to the ageing of PV modules [4]. There are also several visible Non-Current Carrying (NCC) metals or conducting parts of PV panel, which do not carry any current during the normal operation. But, there is a potential risk of electrical hazard when these NCC metals come in contact with the current carrying conductors [3].

The energy produced by the PV system reduces drastically due to faulty and partially shaded conditions [5]. Annually, around 10–20 % of the output power is lost due to partial shading conditions of the PV array [6]. Due to partial shading, some of the cells in PV mod-

ule operate in reverse bias and reach their breakdown voltage [6]. The power loss due to the partial shading may be reduced by using the bypass diodes. Again, the failure of bypass diode causes mismatching of PV modules, leading to the power loss. Also, the failure of bypass diode raises the surface temperature of the PV cell enough to cause fire [7]. Due to the increase in temperature, the thermal power dissipates by the PV cells, which may result in a hotspot problem [6]. Similarly, when an open circuit fault occurs in any single string, the whole string gets disconnected causing the reduction in the output power of the PV array [8]. Also, due to the working of some of the cells in dark conditions, the bypass diode gets activated, causing the reduction of the output voltage of the PV array [8].

The line to line fault (or short circuit fault) decreases the output voltage and it depends on the occurrence of fault between the modules of same string or parallel strings [9]. The open circuit fault in a string reduces the output current, whereas the line to ground fault, short circuit fault and failure of bypass diode reduces the output voltage, thus, leading to the decrease in the output power [10]. So, it may be observed that the decrease in the output voltage or current depends on the type of fault occurred in a PV array.

The faults in PV system may be detected by monitoring its performance and previously recorded data [11]. In order to have a reliable, efficient and safe operation, the protection devices like overcurrent protection device, arc-fault circuit interrupters and ground fault protection device are employed in PV arrays [5]. The protection devices employed in PV system are generally not able to clear the faults during the non-uniform irradiation conditions and night to day transition [10]. Though the chance of the occurrence of different types of faults is very small, the open circuit and short circuit faults occur frequently [10]. The temporary faults like shading due to the buildings, trees, etc., may be cleared within a short period of time, but the permanent faults like electrical disconnection, wiring losses and ageing may not be cleared within the short period of time [12].

The MPPT controller has been designed to drive the PV array at maximum output power at any operating conditions [1] and [10]. It also helps in protecting the power electronic devices by reducing the fault current during faulty conditions. So many MPPT techniques can be found in the literature. These have been implemented to drive the PV array at Maximum Power Point (MPP) under partially shaded conditions or mismatch conditions (one of the fault conditions). But the performance of MPPT techniques during the faulty conditions of PV array has not been found in the literature except the partially shaded conditions.

In this paper, an attempt has been made to analyze the performance of MPPT under fault conditions in terms of MPP tracked, tracking time and tracking efficiency. The implemented MPPT techniques are Perturb & Observe (P&O) method, Incremental Conductance (INC) method and Fuzzy Logic Controller (FLC) method, whereas the studied fault conditions are Open Circuit (OC) fault, Line to Ground (LG), Line to Line (LL) and breakdown of a Bypass Diode (BD). The rest of the paper is organized as follows. Section 2. explains the modelling of the PV module. The MPPT techniques are explained in Sec. 3. Implementation of faults and the results are discussed in Sec. 4. followed by the conclusion.

2. Modeling of PV Module

The PV cell converts the solar energy into the electrical energy. The energy conversion process of the PV module may be realized electrically by using a single diode [13] or two diode equivalent models [14]. The single diode model as shown in Fig. 1 has been considered for the simulation in the presented work, because it is easier to implement and has low complexity when compared to the two-diode model.
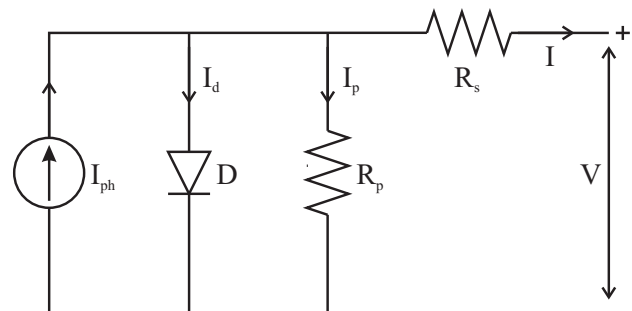

Fig. 1: Single-diode model.

At the output terminals of PV module, the current I [13] may be expressed by Eq. (1).

$$I = I_{ph} - I_d - I_{ps}, \tag{1}$$

where I_d and I_{ps} in (A) are the currents flowing through diode shunt resistance. The current due to incident photon energy I_{ph} in (A) is given by Eq. (2).

$$I_{ph} = (I_{sc,n} + K_I dT)\frac{G}{G_n}. \tag{2}$$

$I_{sc,n}$ is the short circuit current at nominal conditions of 1000 (W·m^{-2}) and 25 (°C). K_I is the short circuit current temperature coefficient. The dT, expressed as d$T = T - T_n$, is the difference between the

operating temperature T and nominal temperature T_n in (K). G and G_n in (W·m^{-2}) are the irradiations at the normal operating condition and nominal condition. The current flowing through the diode is expressed as in Eq. (3):

$$I_d = I_0 \left[\exp \left(\frac{V + IR_S}{V_t a} \right) - 1 \right]. \qquad (3)$$

I_0 in (A) is the diode reverse saturation current and the V in (V) is the output voltage of PV module. The diode ideality factor will be represented by a and its value lies in the range of 1 to 2. R_S in (Ω) is the series resistance of the PV module. The thermal voltage V_t in (V) of the PV module is given by Eq. (4):

$$V_t = \frac{N_S k T}{q}, \qquad (4)$$

where N_S represents the number of series cells in a PV module. k is the Boltzmann constant (1.3806503 · 10^{-23} J·K^{-1}) and q is the charge of the electron (1.60217646·10^{-19} C). The I_0 is expressed as in Eq. (5):

$$I_0 = I_{0,n} \left(\frac{T_n}{T} \right) \exp \left[\frac{q E_g}{a k} \left(\frac{1}{T_n} - \frac{1}{T} \right) \right]. \qquad (5)$$

E_g in (V) stands for the bandgap energy of the p-n junction material and its value is 1.12 eV for polycrystalline silicon at 25 °C. $I_{0,n}$ in (A) is the diode reverse saturation current and is expressed as in Eq. (6):

$$I_{0,n} = \frac{I_{sc,n}}{\exp \left(\frac{V_{oc,n}}{a V_{t,n}} \right) - 1}. \qquad (6)$$

$V_{oc,n}$ and $V_{t,n}$ in (V) are the open circuit voltage and thermal voltage at nominal conditions. The current in shunt resistance is represented as in Eq. (7):

$$I_{ps} = \frac{V + IR_S}{R_P}. \qquad (7)$$

3. Maximum Power Point Tracking Techniques

The Maximum Power Point (MPP) Tracking (MPPT) controller will help in yielding the maximum power from the PV array at any environmental conditions. It consists of a DC-DC converter and an MPPT technique. The DC-DC converter will increase or decrease the PV array output voltage depending on the application. Buck, boost, buck-boost, cuk and sepic are the existing topologies found in the literature [15]. Boost converter suitable for connecting the PV array with grid and for high voltage applications has been implemented in this paper.

The purpose of the MPPT technique is to compute the suitable duty cycle for controlling the switch present in the converter. To drive the PV array at maximum power, the value of duty cycle should be in such a manner that the resistance offered by the PV array at normal operating conditions should be equal to the connected load resistance. The relationship between the resistance offered by the PV array R_P in (Ω), connected load resistance R_L in (Ω) and duty cycle d_o is given by Eq. (8) [16].

$$R_P = R_L (1 - d_o)^2. \qquad (8)$$

The implemented MPPT techniques will be discussed in brief in the following section.

3.1. P&O Method

P&O is one of the most commonly used techniques, because of its simplicity and ease of implementation. The current and voltage of PV array at the initial instant & previous instant is measured and the power at these instants is computed. The ratio of change in power to the change in voltage is calculated at each and every instant as in Eq. (9) [17] and [18].

$$\frac{\mathrm{d}P}{\mathrm{d}V} = \frac{P(n) - P(n-1)}{V(n) - V(n-1)}. \qquad (9)$$

The $P(n)$ and $P(n-1)$ are the powers in (W) at present and previous instants respectively, whereas, the $V(n)$ and $V(n-1)$ in (V) are the voltages at the present and previous instant. Further, the operating voltage of the PV array is increased by perturbing the duty cycle with a small value. If $\mathrm{d}P/\mathrm{d}V > 0$, then the perturbation of duty cycle continues in the same direction, which increases the operating voltage of the PV array to track MPP.

If $\mathrm{d}P/\mathrm{d}V < 0$, then it indicates that the operating voltage is away from the MPP and the duty cycle is perturbed in such a manner that its value decreases causing the operating voltage to decrease further for tracking the MPP. The tracking speed depends on the size of the perturbation value. The tracking speed is faster with the larger perturbation value. The demerits of P&O method are that it fails to track the MPP and depending upon the size of the perturbation value, there are huge oscillations at MPP causing the power loss.

3.2. INC Method

In INC method, the operating point depends on the present value and incremental value of conductance. The ratio of change in current to the change in voltage

is calculated at each and every instant by measuring the present value and the previous value of voltages $V(n)$ & $V(n-1)$ in (V) and currents $I(n)$ & $I(n-1)$ in (A). The slope of the PV curve is represented by the relationship between the initial value and incremental value of conductance. The slope of the PV curve at MPP is zero, whereas it is positive before MPP and is negative after MPP. The MPP is tracked by the INC method by comparing the current value of conductance with its incremental value [19] and is given by the expressions from Eq. (10) to Eq. (13) [17].

$$\frac{\mathrm{d}P}{\mathrm{d}V} = \frac{\mathrm{d}(IV)}{\mathrm{d}V} = I + V\frac{\mathrm{d}I}{\mathrm{d}V} = 0. \tag{10}$$

The Eq. (10) may be expressed as:

$$\frac{\mathrm{d}I}{\mathrm{d}V} = -\frac{I}{V}; \quad \text{at MPP}, \tag{11}$$

$$\frac{\mathrm{d}I}{\mathrm{d}V} > -\frac{I}{V}; \quad \text{before MPP}, \tag{12}$$

$$\frac{\mathrm{d}I}{\mathrm{d}V} < -\frac{I}{V}; \quad \text{after MPP}. \tag{13}$$

The advantage of the INC method is that the optimal value of MPP is tracked at any irradiation conditions, but the tracking rate and efficiency depend on the size of the incremental value.

3.3. FLC Method

FLC is simple non-linear controller and it does not require the plant's mathematical model and technical specifications [20]. Mamdani and Tagachi-Sukeno are the two design approaches available, out of which Mamdani based FLC has been implemented in this paper because of its simplicity and low complexity. The three stages in FLC are fuzzification, rule inference and defuzzification. Fuzzification converts the input crisp values to fuzzy values and defuzzification converts the fuzzy values obtained from the rule inference into output crisp values. A total of 25 rules has been framed in a rule inference system based on the concept of 'if-then' as given in Tab. 1. In Tab. 1, NE stands for negative high, NF for negative small, ZR for zero, PF for positive small and PE for positive high. The three stages of FLC have been realized by using triangular membership functions.

FLC has been implemented in MPPT controller in the place of earlier mentioned methods. The inputs to the FLC are the error 'er' and change in error 'der', given by the equations Eq. (14) and Eq. (15), whereas, duty cycle 'd_o' is the output.

$$er = \frac{\mathrm{d}P}{\mathrm{d}V}. \tag{14}$$

Tab. 1: Rules of FLC.

		der				
		NE	NF	ZR	PF	PE
er	NE	NE	NE	NF	NF	ZR
	NF	NE	NF	NF	ZR	PF
	ZR	NF	NF	ZR	PF	PF
	PF	NF	ZR	PF	PF	PE
	PE	ZR	PF	PF	PE	PE

$$der = \frac{\mathrm{d}P}{\mathrm{d}V}(n) - \frac{\mathrm{d}P}{\mathrm{d}V}(n-1). \tag{15}$$

The 'er' is the differentiation of power with respect to voltage and 'der' is the difference in errors at n^{th} and $(n-1)^{\mathrm{th}}$ position. The output in defuzzification is computed by using the Center of the Area (COA) method.

4. Simulation and Results

A PV array having 12 series connected modules in a string and 5 parallel strings with an output power of 11.68 kW has been simulated to study the tracking of MPP at the time of faults. The KC200GT PV module as in [13] has been selected for simulation. To drive the PV array at MPP, boost converter, best for high voltage applications has been selected. It has a filter component of 7.272 mH and a DC link capacitance of 500 μF. The P&O, INC and FLC are the MPPT techniques implemented to track MPP under the fault conditions of the PV array. A small value (also called perturbation value) of 0.01 has been used as the increment or decrement value of duty cycle in the INC and P&O methods. The faults that have been considered for the simulation are shown in Fig. 2.

The OC fault has been considered in string 1, between the modules 3 & 4 and only this condition has been taken. The OC fault may be considered between any two modules of the same string and it may be observed that the response obtained will remain same. Whereas, the LG fault, that has been applied in string 1 between the modules 5 & 6 has been considered as LG-case-1, between the modules 8 & 9 has been considered as LG-case-2 and between the modules 11 & 12 has been considered as LG-case-3 as shown in Fig. 2.

The LL fault, that has been applied as a line connecting the modules 1 & 2 of string 1 and the modules 1 & 2 of string 2 has been considered as an LL-case-1, whereas the line connecting the modules 1 & 2 of string1 and 6 & 7 of the string 2 has been considered as an LL-case-2.

Failure of bypass diode of module 1 in string 3 has been considered as a BD-case-1, the combination of the failure of bypass diode of modules 1 & 2 of string 3 has
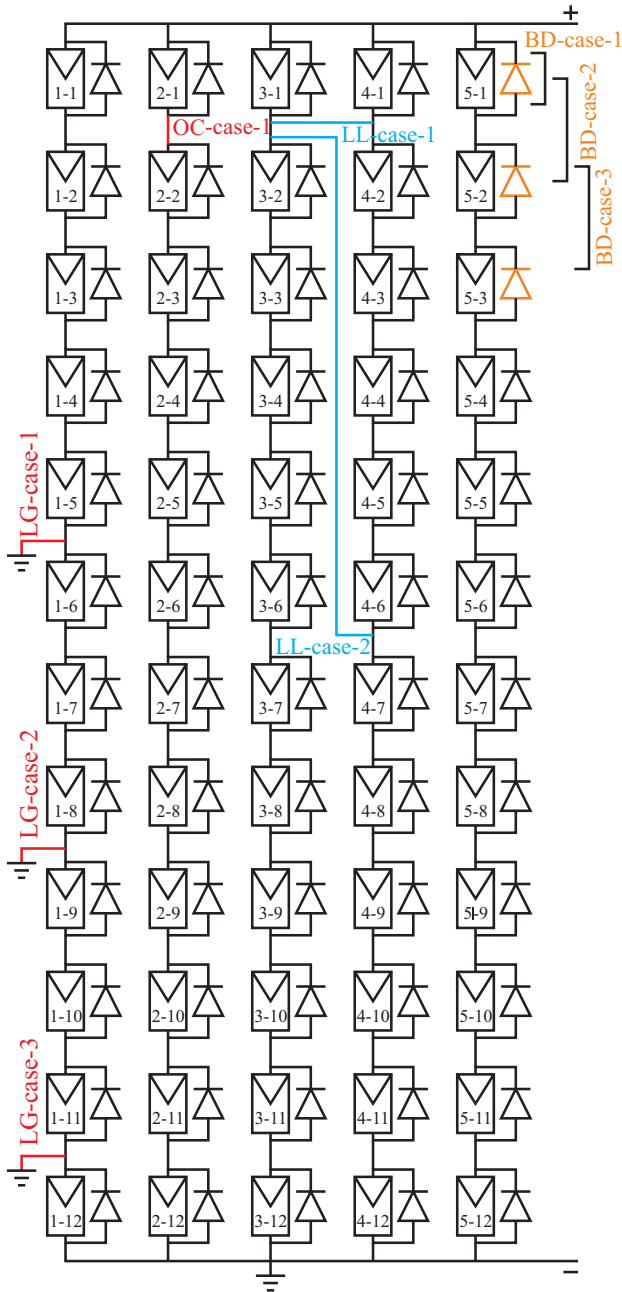
Fig. 2: Faults in a PV array.

Fig. 3: I-V characteristics.

Fig. 4: P-V characteristics.

Tab. 2: MPP under fault conditions and voltage at MPP as per P-V characteristics.

Type of Fault	Different conditions	Max. output power (W)	Voltage at MPP (V)
Nominal	Nominal Condition	11680	311
OC	OC-case-1	9,341	311
LG	LG-case-1	5,619	150.6
	LG-case-2	8,936	239.7
	LG-case-3	11,380	303.5
LL	LL-case-1	11,680	311
	LL-case-2	7,850	210.5
BD	BD-case-1	11,380	303.5
	BD-case-2	10,810	289
	BD-case-3	9,956	267.2

been considered as a BD-case-2 and the combination of the failure of bypass diode of modules 1, 2 & 3 has been considered as a BD-case-3. Under these fault conditions the I-V and P-V characteristics of the PV array are shown in Fig. 3 and Fig. 4. The MPP of the PV array and voltage at MPP under these fault conditions are given in Tab. 2.

From Tab. 2, it may be observed for each type of faults, there are different values of output power. The response of the MPPT controller for each of these fault conditions is shown in Fig. 5, Fig. 6, Fig. 7, Fig. 8, Fig. 9, Fig. 10, Fig. 11, Fig. 12 and Fig. 13. In all the cases of fault, the PV array will be operating un-
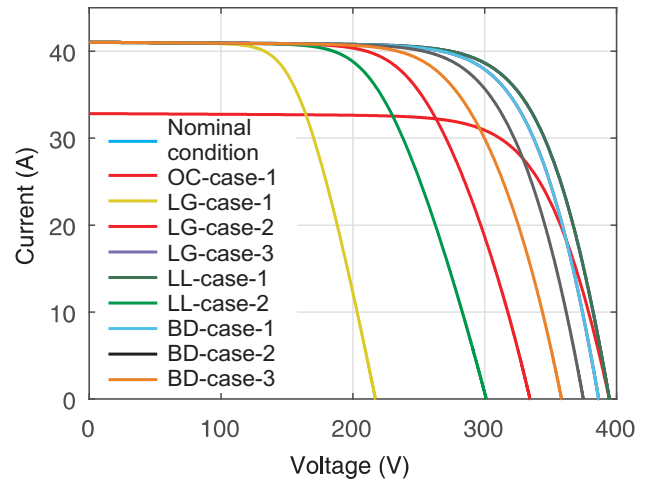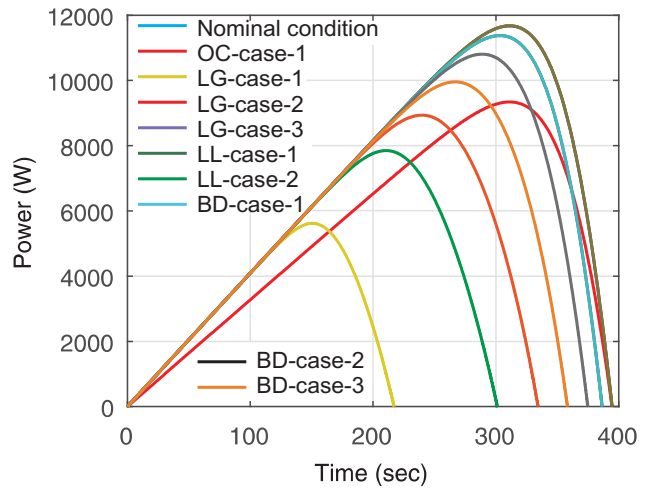
der nominal conditions from 0 to 0.8 s, whereas it is assumed that the fault will occur at 0.8 s and thereafter the PV array will continue to operate under faulty condition.

In Fig. 5, it may be observed that the PV array is operated under nominal conditions from 0 to 0.8 s, whereas, it is operating under OC fault condition from
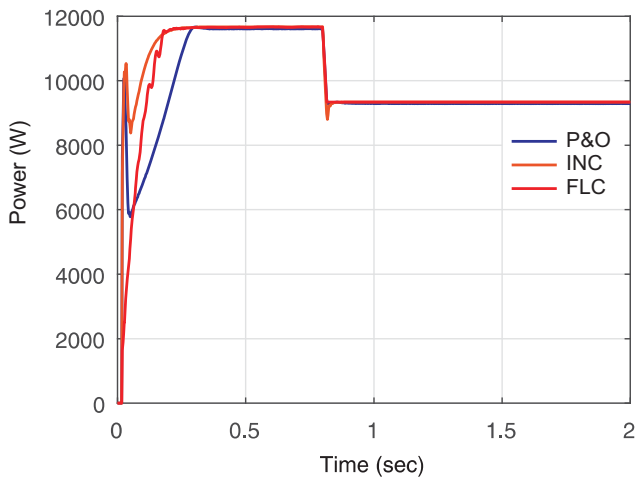
Fig. 5: Power comparison of OC-case-1.

Fig. 7: Power comparison of LG-case-2.
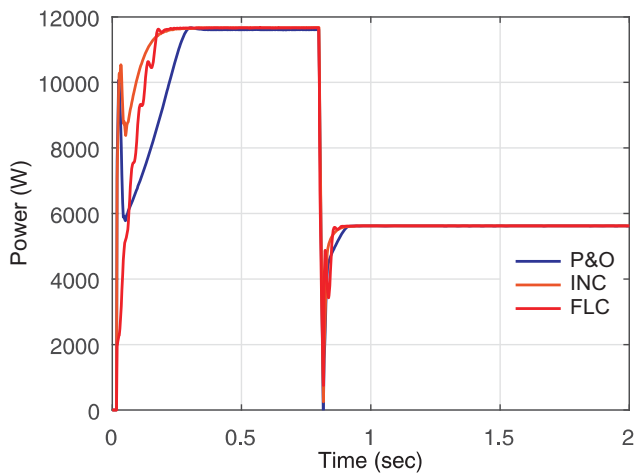

Fig. 6: Power comparison of LG-case-1.

Fig. 8: Power comparison of LG-case-3.

0.8 to 2 s. The power tracked by various MPPT algorithms under the nominal and OC fault conditions was approximately equal to the maximum value with different tracking time. Under nominal conditions, the power tracked by the P&O method was 11,610 W with a tracking time of 0.34 s, INC method was 11,660 W with a tracking time of 0.32 s and FLC method was 11,670 W with a tracking time of 0.27 s.

During the OC fault condition, the P&O method tracks a power of 9,292 W with a tracking time of 0.14 s, INC method tracks a power of 9,336 W with a tracking time of 0.08 s and FLC method tracks a power of 9,340 W with a tracking time of 0.02 s. During the OC fault condition, the voltage at which MPP occurs remains same as that of voltage under nominal condition and the same may be observed from Tab. 2 and Tab. 4. The output current of PV array decreases at the time of OC fault, due to the outage of faulty string.

The power tracked by the MPPT algorithms under nominal conditions remains same for all types of faults.
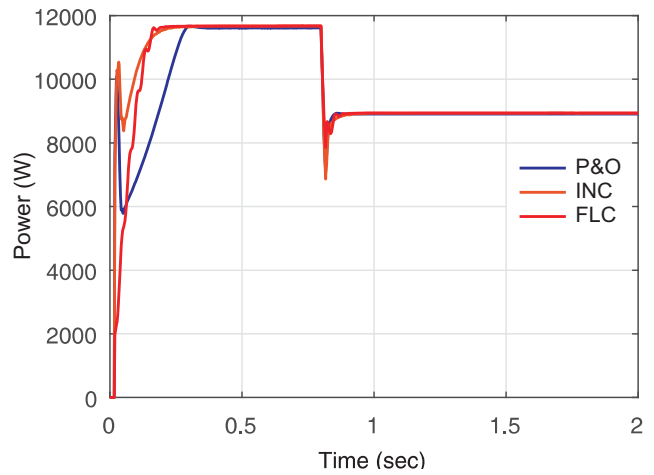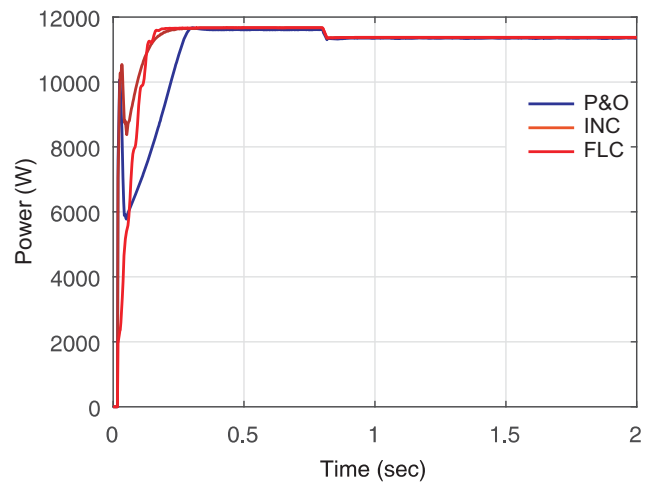
When the fault LG-case-1 occurs on the PV array as shown in Fig. 6, the power tracked by the P&O, INC and FLC methods have had the same value equal to that of 5,620 W with a tracking time of 0.14 s, 0.15 s and 0.11 s respectively. During the fault LG-case-2, a power of 8,905 W has been tracked by the P&O algorithm with a tracking time of 0.09 s, 8,929 W by INC method with a tracking time of 0.17 s and 8,936 W by FLC method with a tracking time of 0.14 s as shown in Fig. 7. During the fault LG-case-3, the power tracked by the P&O method was 11,350 W with a tracking time of 0.1 s, 11,370 W by the INC method with a tracking time of 0.04 s and 11,370 W with a tracking time of 0.02 s as shown in Fig. 8. Hence, from the results of LG faults, it may be observed that there has been a decrease in the output power of the PV array due to decrease in its output voltage.

During the fault condition LL-case-1, the power tracked by the P&O, INC and FLC methods have been the same as that of the power tracked under the nominal conditions as shown in Fig. 9. When the fault
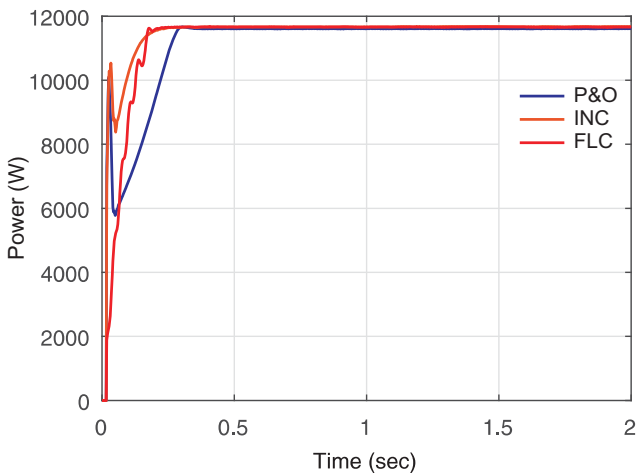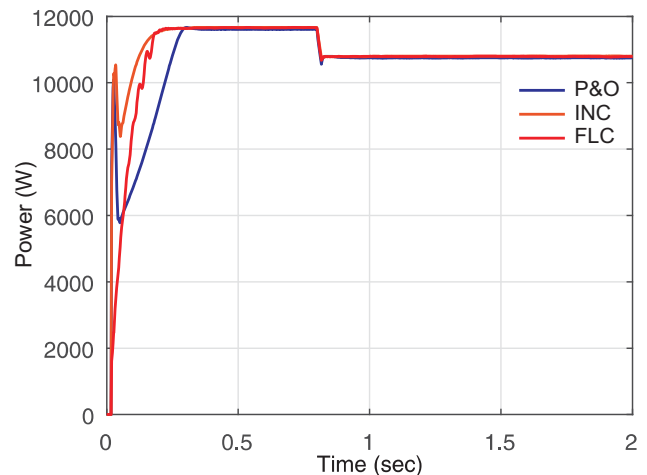
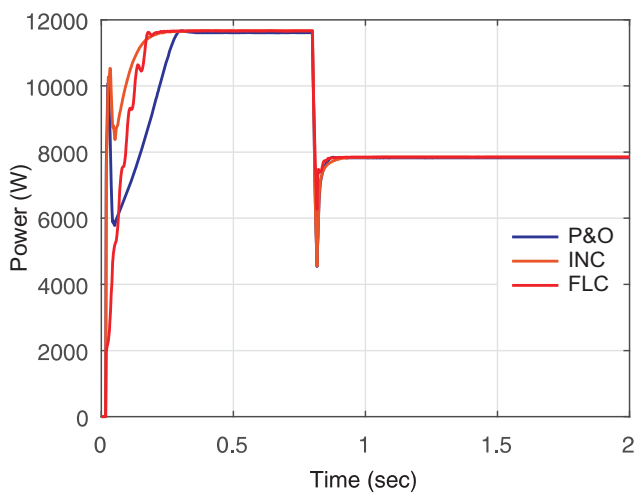**Fig. 9:** Power comparison of LL-case-1.

Fig. 10: Power comparison of LL-case-2.

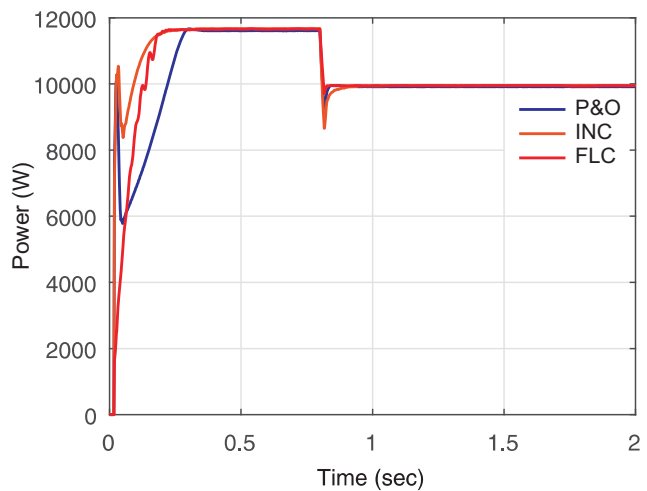**Fig. 11:** Power comparison of BD-case-1.

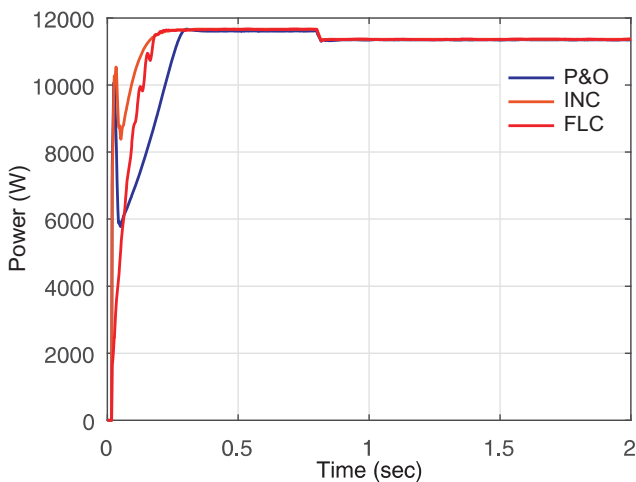**Fig. 12:** Power comparison of BD-case-2.

Fig. 13: Power comparison of BD-case-3.

LL-case-2 occurs on the PV array, the power tracked by the P&O algorithm is 7,826 W with a tracking time of 0.14 s, whereas, the power tracked by the INC and FLC methods was 7,850 W with a tracking time of

0.24 s and 0.12 s respectively as shown in Fig. 10. The results of LL faults reflects the similar scenario as that of LG fault.

For the fault BD-case-1, a power of 11,340 W has been tracked by the P&O method with a tracking time of 0.1 s, 11,370 W tracked by the INC and FLC methods with a tracking time of 0.05 s and 0.02 s as shown in Fig. 11.

During the fault BD-case-2 as shown in Fig. 12, 10,750 W of power has been tracked by the P&O method with a tracking time of 0.09 s, 10,800 W of power has been tracked by the INC and FLC methods with a tracking time of 0.04 s and 0.03 s respectively. When the fault BD-case-3 occurs on a PV array, the power tracked by the P&O algorithm has been 9,916 W with a tracking time of 0.14 s, a power of 9,954 W has been tracked by the INC and FLC methods with a tracking time of 0.3 and 0.05 s respectively as shown in Fig. 13. The results of BD faults also reflect the similar scenario as that of LG faults and LL faults.

Tab. 3: MPP under fault conditions.

Type of Fault	P_{max} (W)	MPPT algorithm	Tracked power (W)	Tracking Efficiency (%)
Nominal Condition	11,680	P&O	11,610	99.4
		INC	11,660	99.8
		FLC	11,670	99.9
OC-case-1	9,341	P&O	9,292	99.47
		INC	9,336	99.94
		FLC	9,340	99.98
LG-case-1	5,620	P&O	5,620	100
		INC	5,620	100
		FLC	5,620	100
LG-case-2	8,936	P&O	8,905	99.65
		INC	8,929	99.92
		FLC	8,936	100
LG-case-3	11,380	P&O	11,350	99.74
		INC	11,370	99.9
		FLC	11,370	99.9
LL-case-1	11,680	P&O	11,610	99.4
		INC	11,660	99.82
		FLC	11,670	99.9
LL-case-2	7,850	P&O	7,826	99.7
		INC	7,850	100
		FLC	7,850	100
BD-case-1	11,380	P&O	11,340	99.65
		INC	11,370	99.9
		FLC	11,370	99.9
BD-case-2	10,810	P&O	10,750	99.44
		INC	10,800	99.9
		FLC	10,800	99.9
BD-case-3	9,956	P&O	9,916	99.6
		INC	9,954	99.97
		FLC	9,954	99.97

Tab. 4: Tracking time along with output voltage and current.

Type of Fault	MPPT algorithm	Tracking time (s)	Output voltage (V)	Output current (A)
Nominal Condition	P&O	0.34	311	37.33
	INC	0.32	314.2	37.11
	FLC	0.27	308.75	37.8
OC-case-1	P&O	0.14	311	29.88
	INC	0.08	313.9	29.74
	FLC	0.02	306	30.52
LG-case-1	P&O	0.14	150.65	37.3
	INC	0.15	151.25	37.16
	FLC	0.1	150.9	37.25
LG-case-2	P&O	0.09	239.4	37.2
	INC	0.17	243	36.75
	FLC	0.14	240.7	37.13
LG-case-3	P&O	0.1	303	37.46
	INC	0.05	306.9	37.05
	FLC	0.02	304	37.41
LL-case-1	P&O	0.34	311	37.33
	INC	0.32	314.2	37.11
	FLC	0.27	308.75	37.8
LL-case-2	P&O	0.14	210.6	37.16
	INC	0.24	211.4	37.13
	FLC	0.12	211	37.21
BD-case-1	P&O	0.1	304	37.3
	INC	0.05	307.3	37.04
	FLC	0.02	300.5	37.84
BD-case-2	P&O	0.09	288.3	37.29
	INC	0.04	286.4	37.71
	FLC	0.03	286.7	37.67
BD-case-3	P&O	0.14	266.2	37.25
	INC	0.3	268.8	37.03
	FLC	0.05	266.15	37.4

From the figures and Tab. 3, it may be observed that the power tracked by the INC and FLC methods has been approximately equal, but the tracking time of MPP is very short in FLC when compared to the INC method. Also from Tab. 4, it may be observed that the operating voltage at MPP under fault conditions is almost equal to the voltage at MPP obtained from the P-V characteristics as given in Tab. 2. In Tab. 4, the decrease in the output voltage may be observed in the simulated fault conditions except the OC fault, but the change in the output current of PV array has been very minimal.

The tracking efficiency of MPPT algorithms at the time of fault is given in Tab. 3. In Tab. 3, it may be observed that the tracking efficiency of FLC method was better when compared to the other two methods.

Hence, it may be concluded that the performance of FLC method has been more efficient at the time of faults on PV array.

5. Conclusion

The performance of MPPT algorithms during the fault conditions have been analyzed by using a PV array of 11.68 kW with 12×5 arrangement. The faults like open circuit fault, line to ground fault, line to line fault and bypass diode fault have been considered. Again, in these faults, different cases, which are possible for the simulation has been implemented. In this analysis, it has been found that the FLC method is quite good at tracking the maximum power under any conditions of operation. The tracking time is shorter and tracking efficiency is higher when compared to the other methods. Though the INC method is also tracking the MPP approximately equally to that of FLC method, but the tracking time is shorter.

References

[1] ZHAO, Y., J. F. D. PALMA, M. JERRY, L. J. ROBERT and L. BRAD. Line-Line Fault Analysis and Protection Challenges in Solar Photovoltaic Arrays. *IEEE Transactions on Industrial Electronics*. 2013, vol. 60, iss. 9, pp. 3784–3795. ISSN 0278-0046. DOI: 10.1109/TIE.2012.2205355.

[2] YI, Z. and A. H. ETEMADI. Fault Detection for Photovoltaic Systems Based on Multi-Resolution Signal Decomposition and Fuzzy Inference Systems. *IEEE Transactions on Smart Grid*. 2017,

vol. 8, iss. 3, pp. 1274–1283. ISSN 1949-3053. DOI: 10.1109/TSG.2016.2587244.

[3] ALAM, M. K., F. KHAN, J. JOHNSON and J. FLICKER. A Comprehensive Review of Catastrophic Faults in PV Arrays: Types, Detection, and Mitigation Techniques. *IEEE Journal of Photovoltaics.* 2015, vol. 5, iss. 3, pp. 982–997. ISSN 2156-3381. DOI: 10.1109/JPHOTOV.2015.2397599.

[4] CHAO, K. H. and C. T. CHEN. A remote supervision fault diagnosis meter for photovoltaic power generation systems. *Measurement.* 2017, vol. 104, iss. 1, pp. 93–104. ISSN 0263-2241. DOI: 10.1016/j.measurement.2017.03.017.

[5] HARIHARAN, R., M. CHAKKARAPANI, G. S. ILANGO and C. NAGAMANI. A Method to Detect Photovoltaic Array Faults and Partial Shading in PV Systems. *IEEE Journal of Photovoltaics.* 2016, vol. 6, iss. 5, pp. 1278–1285. ISSN 2156-3381. DOI: 10.1109/JPHOTOV.2015.2397599.

[6] BRESSAN, M., Y. E. BASRI, A. G. GALEANO and C. ALONSO. A shadow fault detection method based on the standard error analysis of I-V curves. *Renewable Energy.* 2016, vol. 99, iss. 1, pp. 1181–1190. ISSN 0960-1481. DOI: 10.1016/j.renene.2016.08.028.

[7] KO, S. W., Y. C. JU, H. M. HWANG, J. H. SO, Y. S. JUNG, H. J. SONG, H. E. SONG, S. H. KIM and G. H. KANG. Electric and thermal characteristics of photovoltaic modules under partial shading and with a damaged bypass diode. *Energy.* 2017, vol. 128, iss. 1, pp. 232–243. ISSN 0360-5442. DOI: 10.1016/j.energy.2017.04.030.

[8] SILVESTRE, S., M. A. D. SILVA, A. CHOUDER, D. GUASCH and E. KARATEPE. New procedure for fault detection in grid connected PV systems based on the evaluation of current and voltage indicators. *Energy Conversion and Management.* 2014, vol. 86, iss. 1, pp. 241–249. ISSN 0196-8904. DOI: 10.1016/j.enconman.2014.05.008.

[9] ARANI, M. S. and M. A. HEJAZI. The comprehensive study of electrical faults in PV arrays. *Journal of Electrical and Computer Engineering.* 2016, vol. 2016, ID 8712960, pp. 1–10. ISSN 2090-0147. DOI: 10.1155/2016/8712960.

[10] HAZRA, A., S. DAS and M. BASU. An efficient fault diagnosis method for PV systems following string current. *Journal of Cleaner Production.* 2017, vol. 154, iss. 1, pp. 220–232. ISSN 0959-6526. DOI: 10.1016/j.jclepro.2017.03.214.

[11] FIRTH, S. K., K. J. LOMAS and S. J. REES. A simple model of PV system performance and its use in fault detection. *Solar Energy.* 2010, vol. 84, iss. 4, pp. 624–635. ISSN 0038-092X. DOI: 10.1016/j.solener.2009.08.004.

[12] MADETI, S. R. and S. N. SINGH. Online fault detection and the economic analysis of grid-connected photovoltaic systems. *Energy.* 2017, vol. 134, iss. 1, pp. 121–135. ISSN 0360-5442. DOI: 10.1016/j.energy.2017.06.005.

[13] VILLALVA, M. G., J. R. GAZOLI and E. R. FILHO. Comprehensive Approach to Modeling and Simulation of Photovoltaic Arrays. *IEEE Transactions on Power Electronics.* 2009, vol. 24, iss. 5, pp. 1198–1208. ISSN 0885-8993. DOI: 10.1109/TPEL.2009.2013862.

[14] ISHAQUE, K., Z. SALAM, H. TAHERI and SYAFARUDDIN. Modeling and simulation of photovoltaic (PV) system during partial shading based on a two-diode model. *Simulation Modelling Practice and Theory.* 2011, vol. 19, iss. 1, pp. 1613–1626. ISSN 1569-190X. DOI: 10.1016/j.simpat.2011.04.005.

[15] TAGHVAEE, M. H., M. A. M. RADZI, S. M. MOOSAVAIN, H. HIZAM and M. H. MARHABAN. A current and future study on non-isolated DC-DC converters for photovoltaic applications. *Renewable and Sustainable Energy Reviews.* 2013, vol. 17, iss. 1, pp. 216–227. ISSN 1364-0321. DOI: 10.1016/j.rser.2012.09.023.

[16] BASOGLU, M. E. and B. CAKIR. Comparisons of MPPT performances of isolated and non-isolated DC-DC converters by using a new approach. *Renewable and Sustainable Energy Reviews.* 2016, vol. 60, iss. 1, pp. 1100–1113. ISSN 1364-0321. DOI: 10.1016/j.rser.2016.01.128.

[17] SARAVANAN, S. and N. R. BABU. Maximum power point tracking algorithms for photovoltaic system - A review. *Renewable and Sustainable Energy Reviews.* 2016, vol. 57, iss. 1, pp. 192–204. ISSN 1364-0321. DOI: 10.1016/j.rser.2015.12.105.

[18] FEMIA, N., G. PETRONE, G. SPAGNUOLO and M. VITELLI. Optimization of Perturb and Observe Maximum Power Point Tracking Method. *IEEE Transactions on Power Electronics.* 2005, vol. 20, iss. 4, pp. 963–973. ISSN 0885-8993. DOI: 10.1109/TPEL.2005.850975.

[19] ELTAWIL, M. A. and Z. ZHAO. MPPT techniques for photovoltaic applications. *Renewable and Sustainable Energy Reviews.* 2013, vol. 25, iss. 1, pp. 793–813. ISSN 1364-0321. DOI: 10.1016/j.rser.2013.05.022.

[20] SEYEDMAHMOUDIAN, M., B. HORAN, T. K. SOON, R. RAHMANI, A. M. T. OO, S. MEKHILEF and A. STOJCEVSKI. State of the art artificial intelligence-based MPPT techniques for mitigating partial shading effects on PV systems - A review. *Renewable and Sustainable Energy Reviews*. 2016, vol. 64, iss. 1, pp. 435–455. ISSN 1364-0321. DOI: 10.1016/j.rser.2016.06.053.

About Authors

Krishna Naick BHUKYA is working as an Assistant Professor in Department of Electrical Engineering at Indian Institute of Technology (Indian School of Mines), Dhanbad, Jharkhand, India. His research interests include Renewable Energy Sources.

Kalyan CHATTERJEE is working as an Associate Professor in Department of Electrical Engineering at Indian Institute of Technology (Indian School of Mines), Dhanbad, Jharkhand, India. His research interests include Soft Computing Applications in Power System.

Tarun Kumar CHATTERJEE is working as a Professor in Department of Mining Machinery Engineering at Indian Institute of Technology (Indian School of Mines), Dhanbad, Jharkhand, India. His research interests include Mine Electrical Equipments.